

surface is low (7), so that strain fields introduced by unpaired DBs may not be effectively screened.

The DB diffusional dynamics reported here has important implications for surface processes and, in particular, materials growth. It demonstrates that at low temperatures, because of an attractive interaction, a majority of DB sites are likely to be paired and hence available for dissociative chemisorption and further growth. Had it been otherwise, growth would necessarily become a trimolecular process involving two uncorrelated surface DBs and an incident precursor molecule. At higher temperatures, entropy drives DBs to unpair, and DB diffusion becomes increasingly random. However, the number of DB sites is correspondingly larger (because of desorption), so that a statistically significant fraction of sites is present in a configuration that favors growth. Although the present study involves the Si(100) surface, these same arguments may well apply to a variety of systems, particularly if through-space DB interactions prove to be the origin of these local correlations.

REFERENCES AND NOTES

1. J. M. Jasinski, B. S. Meyerson, B. A. Scott, *Annu. Rev. Phys. Chem.* **38**, 109 (1987).
2. Y. Suda, D. Lubben, T. Mooka, J. E. Greene, *J. Vac. Sci. Technol. A* **8**, 61 (1990); S. M. Gates, *Surf. Sci.* **195**, 307 (1988).
3. Omicron Vakuumphysik, Taunstein, Germany.
4. J. J. Boland, *Adv. Phys.* **42**, 129 (1993).
5. T.-C. Shen *et al.*, *Science* **268**, 1590 (1995).
6. E. T. Foley *et al.*, *Phys. Rev. Lett.*, in press.
7. J. J. Boland, *ibid.* **67**, 1593 (1991).
8. M. McEllistrem and J. J. Boland, in preparation.
9. These data differ from previous STM studies of DBs on the Si(100)-2 \times 1:H surface after H₂ desorption (7). Specifically, DBs were previously found to largely be paired, whereas the present study shows DBs that unpair and can be frozen in unpaired configurations once T_s is too low for D atoms to diffuse. The different behaviors can be explained by the different thermal treatments used. In the present study, T_s was increased slowly, D₂ was desorbed over a period of several minutes, and the sample was then cooled to the imaging temperature. In the previous study, by contrast, H₂ was desorbed in a rapid anneal-and-quench thermal cycle, and the surface was imaged at room temperature. The rapid method minimizes the time available for the DBs to unpair, resulting in a population of predominantly paired DBs.
10. A. Vittadini, A. Selloni, M. Casarin, *Phys. Rev. B* **49**, 11191 (1994).
11. P. Nachtigall, K. D. Jordan, K. C. Janda, *J. Chem. Phys.* **95**, 8652 (1991); M. P. D. D'Evelyn, Y. L. Yang, L. F. Sutcu, *ibid.* **98**, 3560 (1993); U. Hofer, L. Li, T. F. Heinz, *Phys. Rev. B* **45**, 9485 (1992).
12. G. A. deWijns and A. Selloni, *Phys. Rev. Lett.* **77**, 881 (1996).
13. C. J. Wu and E. A. Carter, *Phys. Rev. B* **46**, 4651 (1992).
14. J. H. G. Owen, D. R. Bowler, C. M. Goringe, K. Miki, G. A. D. Briggs, *ibid.* **54**, 14153 (1996).
15. In an earlier halogen study [J. J. Boland, *Science* **262**, 1703 (1993)], we noted that at room temperature, two Cl atoms that were bonded on neighboring dimers showed a distinct preference to be on the same side of the dimer row. This preference remained even under imaging conditions where single Cl atoms (and unpaired DBs) readily hopped back and forth between sites on the same dimer.

16. A preliminary analysis of hopping rates to determine the relative energies of paired and unpaired configurations indicated that the predissociated configuration is stabilized compared with that of unpaired DBs, although not to the extent of paired DBs.
17. R. J. Hamers and U. K. Koehler, *J. Vac. Sci. Technol. A* **7**, 2854 (1989).

18. We thank E. J. Buehler and M. Fouchier for programming assistance, and M. Rubinstein and J. L. Whitten for insightful discussions. Financial support by NSF under contracts DMR 9509790 and DMR 9413999 is gratefully acknowledged.

26 September 1997; accepted 5 December 1997

Triblock Copolymer Syntheses of Mesoporous Silica with Periodic 50 to 300 Angstrom Pores

Dongyuan Zhao, Jianglin Feng, Qisheng Huo, Nicholas Melosh, Glenn H. Fredrickson, Bradley F. Chmelka,* Galen D. Stucky*

Use of amphiphilic triblock copolymers to direct the organization of polymerizing silica species has resulted in the preparation of well-ordered hexagonal mesoporous silica structures (SBA-15) with uniform pore sizes up to approximately 300 angstroms. The SBA-15 materials are synthesized in acidic media to produce highly ordered, two-dimensional hexagonal (space group *p6mm*) silica-block copolymer mesophases. Calcination at 500°C gives porous structures with unusually large interlattice *d* spacings of 74.5 to 320 angstroms between the (100) planes, pore sizes from 46 to 300 angstroms, pore volume fractions up to 0.85, and silica wall thicknesses of 31 to 64 angstroms. SBA-15 can be readily prepared over a wide range of uniform pore sizes and pore wall thicknesses at low temperature (35° to 80°C), using a variety of poly(alkylene oxide) triblock copolymers and by the addition of cosolvent organic molecules. The block copolymer species can be recovered for reuse by solvent extraction with ethanol or removed by heating at 140°C for 3 hours, in both cases, yielding a product that is thermally stable in boiling water.

Large pore-size molecular sieves are much in demand for reactions or separations involving large molecules (1, 2). Since mesoporous molecular sieves such as hexagonally ordered MCM-41 were discovered by Mobil Corporation scientists in 1992 (3, 4), surfactant-templated synthetic procedures have been extended to include a wide range of compositions, and a variety of conditions have been developed for exploiting the structure-directing functions of electrostatic, hydrogen-bonding, and van der Waals interactions associated with amphiphilic molecules (5–16). Typically, these materials are synthesized under conditions where silica-surfactant self-assembly (16) occurs simultaneously with condensation of the inorganic species, yielding mesoscopically ordered composites. For example, MCM-41 materials prepared with cationic cetyltri-

methylammonium (CTA⁺) surfactants commonly have *d*(100) spacings of about 40 Å, which after calcination yield a hexagonally ordered porous solid with uniform pore sizes of 20 to 30 Å (5–9, 12). Cosolvent organic molecules, such as 1,3,5-trimethylbenzene (TMB) used to expand the pore size of MCM-41 up to 100 Å (3, 4), unfortunately yield materials with less-resolved x-ray diffraction (XRD) patterns, particularly near the high end of this size range, for which a single broad diffraction peak is often observed (9). Extended thermal treatment during synthesis gives expanded pore sizes up to ~50 Å (17). We have used postsynthesis treatment, by subsequently heating the product obtained from an alkaline S⁺I⁻ synthesis at room temperature in distilled water at pH = 7, to obtain pore sizes as large as ~60 Å (9) without the need for organic swelling agents. Using CTA⁺ surfactant species in an L₃ sponge phase, McGrath *et al.* (18) created siliceous solids with large, uniform, but disordered pore assemblies. Pinnavaia and co-workers (11) used nonionic surfactants in neutral aqueous media to synthesize worm-like disordered mesoporous silica with uniform pore sizes of 20 to 58 Å. To increase the dimensions of pore structures produced in such inorganic-organic com-

D. Zhao, Q. Huo, G. D. Stucky, Department of Chemistry and Materials Research Laboratory, University of California, Santa Barbara, CA 93106, USA.

J. Feng, Department of Chemistry and Center for Quantized Electronic Structures, University of California, Santa Barbara, CA 93106, USA.

N. Melosh, G. H. Fredrickson, B. F. Chmelka, Materials Research Laboratory and Department of Chemical Engineering, University of California, Santa Barbara, CA 93106, USA.

*To whom correspondence should be addressed. E-mail: bradc@engineering.ucsb.edu (B.F.C.); stucky@chem.ucsb.edu (G.D.S.)

posite syntheses, we anticipated that the use of amphiphilic polymers of larger molecular weight would extend the mesoscopic-length scales achievable.

We report the syntheses of well-ordered hexagonal mesoporous silica structures (SBA-15) with tunable large uniform pore sizes (up to ~ 300 Å) which are obtained by use of amphiphilic block copolymers (15, 19) as organic structure-directing agents. In particular, poly(alkylene oxide) triblock copolymers such as poly(ethylene oxide)-poly(propylene oxide)-poly(ethylene oxide) (PEO-PPO-PEO) are good candidates, because of their mesostructural ordering properties, amphiphilic character, low-cost commercial availability, and biodegradability. Using aqueous acidic conditions ($\text{pH} \approx 1$) and dilute triblock copolymer concentrations, SBA-15 has been synthesized with a highly ordered (four- to seven-peak XRD pattern) two-dimensional (2D) hexagonal ($p6mm$) mesostructure and thick uniform silica walls (31 to 64 Å). The thick silica walls, in particular, are different from thinner walled MCM-41 structures made with conventional cationic surfactants and lead to greater hydrothermal stability on the part of SBA-15. The pore size and the thickness of the silica wall can be adjusted by varying the heating temperature (35° to 140°C) and time (11 to 72 hours) of SBA-15 in the reaction solution.

SBA-15 can be synthesized over a range of reaction mixture compositions and conditions. Use of concentrations of block copolymer higher than 6 weight % yields only silica gel or produces no precipitation of silica, whereas concentrations of copolymer below 0.5 weight % result in only amorphous silica. Preparation of SBA-15 has been achieved with reaction temperatures between 35° and 80°C. At room temperature, only amorphous silica powder or poorly ordered products are obtained, whereas higher temperatures ($>80^\circ\text{C}$) yield silica gel. Tetraethoxysilane (TEOS), tetramethoxysilane (TMOS), and tetrapropoxysilane (TPOS) are suitable sources of silica for the preparation of SBA-15. Hexagonal mesoporous SBA-15 has been formed in acid media ($\text{pH} < 1$) with HCl, HBr, HI, HNO_3 , H_2SO_4 , or H_3PO_4 acids. At pH values from 2 to 6, above the isoelectric point of silica ($\text{pH} \sim 2$), no precipitation or formation of silica gel occurs. At neutral $\text{pH} \sim 7$, only disordered or amorphous silica is obtained (11, 15).

SBA-15 samples with $d(100)$ spacings in the range 74.5 to 118 Å and pore sizes between 46 and 100 Å have been synthesized by using PEO-PPO-PEO triblock copolymers with different ratios of ethylene oxide (EO) and propylene oxide (PO) compositions with and without addition of

TMB as a swelling agent. For the triblock architectures used, the EO:PO ratio affects the formation of SBA-15, with a lower ratio favoring a $p6mm$ hexagonal morphology. For example, use of Pluronic L121 ($\text{EO}_5\text{PO}_7\text{EO}_5$) (20) at low concentrations (0.5 to 1 weight %) in the absence of cosolvent species leads to hexagonal SBA-15, whereas higher concentrations (2 to 5 weight %) yield an unstable lamellar mesostructured product. Higher EO:PO ratios in the block copolymer, such as $\text{EO}_{106}\text{PO}_{70}\text{EO}_{106}$, $\text{EO}_{100}\text{PO}_{39}\text{EO}_{100}$, or $\text{EO}_{80}\text{PO}_{30}\text{EO}_{80}$, produce cubic mesoporous silica (13, 21). Hexagonal mesoporous silica SBA-15 can also be synthesized by using reversed PPO-PEO-PPO architectures, for example $\text{PO}_{19}\text{EO}_{33}\text{PO}_{19}$. Table 1 summarizes the physicochemical properties of mesoporous silica prepared by using poly(alkylene oxide) triblock and reverse triblock copolymers.

The small-angle XRD pattern for as-synthesized mesoporous silica (SBA-15) prepared with $\text{EO}_{20}\text{PO}_{70}\text{EO}_{20}$ shows four well-resolved peaks (Fig. 1A) that are indexable as (100), (110), (200), and (210) reflections associated with $p6mm$ hexagonal symmetry. Three additional weak peaks in the 2θ range of 1° to 3.5° correspond to the (300), (220), and (310) scattering reflections (3, 4, 9), indicating that as-synthesized SBA-15 has a high degree of hexagonal mesoscopic organization. The intense (100) peak reflects a d spacing of 104 Å,

corresponding to a large unit-cell parameter ($a_0 = 120$ Å) (9). After calcination in air at 500°C for 6 hours, the XRD pattern (Fig. 1B) shows that the $p6mm$ morphology is preserved, although the peaks appear at slightly larger 2θ values, with $d(100) = 95.7$ Å and $a_0 = 110$ Å. Six XRD peaks are still observed, confirming that hexagonal SBA-15 is thermally stable. A similarly high degree of mesoscopic order (four $p6mm$ XRD peaks) is observed for hexagonal SBA-15 even after calcination to 850°C .

Scanning electron microscopy (SEM) images (Fig. 2) reveal that the as-synthesized SBA-15 sample of Fig. 1 consists of many rope-like domains with relatively uniform sizes of ~ 1 μm , which are aggregated into wheat-like macrostructures. After calcination in air at 500°C , SBA-15 shows a similar particle morphology, which reflects the thermal stability of the macroscopic structure. Transmission electron microscopy (TEM) images (Fig. 3) of calcined SBA-15 [including different sample orientations (22)] show well-ordered hexagonal arrays of mesopores (1D channels) and further confirm that SBA-15 has a 2D $p6mm$ hexagonal structure (3, 4, 9). From high-dark contrast in the TEM image of this sample (Fig. 3B), the distance between mesopores is estimated to be ~ 110 Å, in agreement with that determined from the XRD data.

A calcined SBA-15 sample prepared

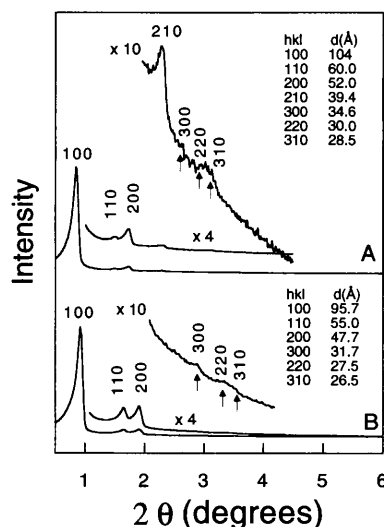


Fig. 1. Powder XRD patterns of (A) as-synthesized and (B) calcined mesoporous silica (SBA-15) prepared using the amphiphilic triblock copolymer $\text{EO}_{20}\text{PO}_{70}\text{EO}_{20}$ as structure-directing species. The chemical composition of the reaction mixture was 4 g copolymer:0.041 mol TEOS:0.24 mol HCl:6.67 mol H_2O . The XRD patterns were acquired on a Scintag PADX diffractometer equipped with a liquid nitrogen-cooled germanium solid-state detector using $\text{Cu K}\alpha$ radiation.

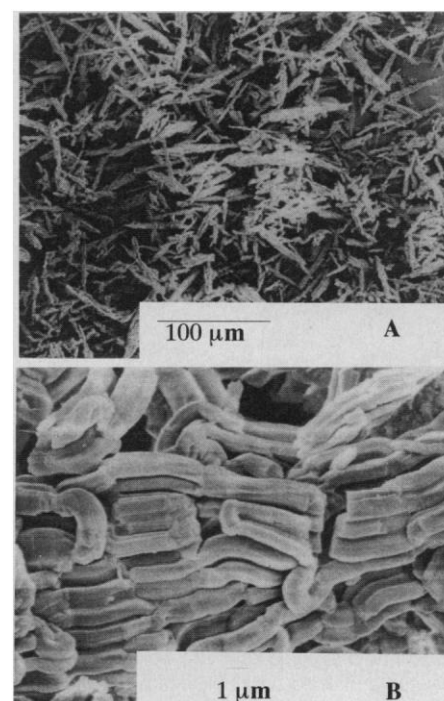


Fig. 2. Scanning electron micrographs of as-synthesized hexagonal mesoporous silica SBA-15 obtained on a JEOL 6300-F microscope at different magnifications.

with $\text{EO}_{20}\text{PO}_{70}\text{EO}_{20}$ by reaction at 35°C for 20 hours, heating at 100°C for 48 hours, and subsequent calcination in air at 500°C , yielded an SBA-15 product with a mean pore size of 89 \AA , a pore volume of $1.17 \text{ cm}^3/\text{g}$, and a Brunauer-Emmett-Teller (BET) surface area of $850 \text{ m}^2/\text{g}$. Three well-distinguished regions of the adsorption isotherm (Fig. 4) are evident: (i) monolayer-multilayer adsorption, (ii) capillary condensation, and (iii) multilayer adsorption on the outer particle surfaces. In contrast to N_2 adsorption results (23, 24) for MCM-41 mesoporous silica with pore sizes $\sim 40 \text{ \AA}$, a clear type-H1 hysteresis loop (23) is observed, and the capillary condensation occurs at a higher relative pressure ($P/P_0 \sim 0.75$). The approximate pore size calculated using the Barrett-Joyner-Halenda analysis (23, 24) is significantly smaller than the repeat distance determined by XRD, using the Halsey equation for multilayer thickness, because the latter includes the thickness of the pore wall. The thickness

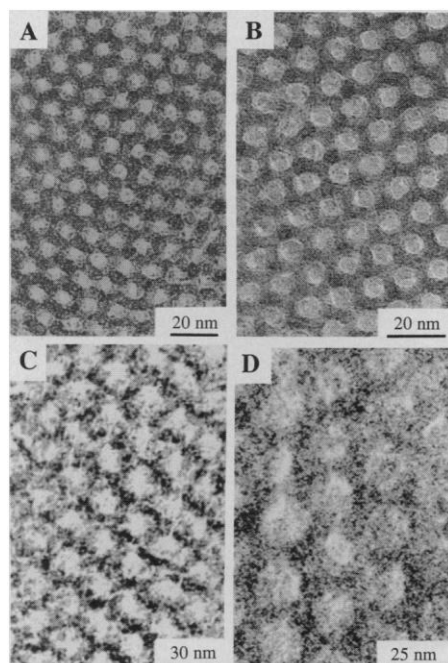


Fig. 3. TEM images of calcined hexagonal SBA-15 mesoporous silica with different average pore sizes, from BET and XRD results (24): (A) 60 \AA , (B) 89 \AA , (C) 200 \AA , and (D) 260 \AA . The thicknesses of the silica walls are estimated to be (A) 53 \AA , (B) 31 \AA , (C) 40 \AA , and (D) 40 \AA . The micrographs were recorded digitally with a Gatan slow-scan charge-coupled device (CCD) camera on a JEOL 2010 electron microscope operating at 200 kV . The samples were prepared by dispersing the powder products as a slurry in acetone, which was then deposited and dried on a holey carbon film on a Cu grid. A low-exposure technique was used to reduce the effect of beam damage and sample drift. Focus-series measurements show that the bright areas correspond to the pores and dark areas to the silica walls.

of the pore wall is estimated to be $\sim 31 \text{ \AA}$ (Table 1) for SBA-15 prepared with $\text{EO}_{20}\text{PO}_{70}\text{EO}_{20}$.

Heating as-synthesized SBA-15 in the reaction solution at different temperatures (80° to 140°C) and for different lengths of time (11 to 72 hours) resulted in a series of structures with systematically different uniform pore sizes (47 to 89 \AA) and different silica wall thicknesses (31 to 64 \AA) (Table 1 and Fig. 3, A and B) (25). These wall structures are substantially thicker than those typical for MCM-41 (commonly 10 to 15 \AA) prepared with alkylammonium cationic surfactant species as structure-directing agents (3, 4, 12). Higher temperatures or longer reaction times result in larger pore sizes and thinner silica walls, which may be caused by protonation or temperature-de-

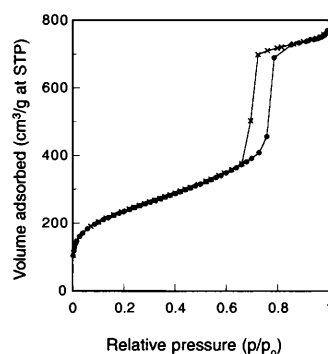


Fig. 4. Nitrogen adsorption (●)–desorption (×) isotherm and pore volume plots for calcined mesoporous silica SBA-15 prepared with the amphiphilic triblock copolymer $\text{EO}_{20}\text{PO}_{70}\text{EO}_{20}$. The isotherms were measured with a Micromeritics ASAP 2000 system. The pore volume was determined from the adsorption branch of the N_2 isotherm curve at the $P/P_0 = 0.983$ signal point. STP, standard temperature and pressure.

pendent hydrophilicity of the PEO block of the copolymer under the acidic synthesis conditions (13, 26), or a combination of both. Resulting PEO moieties are expected to interact more strongly with the silica species and thus be more closely associated with the inorganic wall than the more hydrophobic PPO block. However, at higher temperatures, the PEO blocks become more hydrophobic (26), resulting in increased hydrophobic domain volumes, smaller lengths of PEO segments associated with the silica wall (see below), and increased pore sizes.

The pore size of hexagonal mesoporous SBA-15 can be increased to more than 300 \AA by increasing the hydrophobic volume of the self-assembled aggregates. This can be achieved by changing the copolymer composition or block sizes, or by adding cosolvent organic molecules such as TMB. For example, the XRD pattern of as-synthesized SBA-15 prepared with a TMB: $\text{EO}_{20}\text{PO}_{70}\text{EO}_{20}$ weight ratio of 3:4 (Fig. 5, curve A) shows three peaks with d spacings of 270 , 154 , and 133 \AA at very low angles (2θ range from 0.2° to 1°), which are indexable as (100), (110), and (200) reflections associated with $p6mm$ hexagonal symmetry (4, 6). The intense (100) peak reflects a d spacing of 270 \AA , corresponding to a unit cell parameter a_0 of 310 \AA . After calcination in air at 500°C for 6 hours, the XRD pattern (Fig. 5, curve B) displays slightly improved resolution, with a broad (210) reflection at a d spacing of 100 \AA . In spite of such large lattice dimensions, hexagonal SBA-15 is thermally stable and mesoscopically well ordered: the calcined product has a BET surface area of $910 \text{ m}^2/\text{g}$, an average pore size of 260 \AA , a pore volume of $2.2 \text{ cm}^3/\text{g}$, and TEM images show a highly ordered material

Table 1. Preparation and physicochemical properties of hexagonal SBA-15 prepared with poly(alkylene oxide) triblock copolymers. The value inside brackets for $d(100)$ is the value for the SBA-15 product calcined at 500°C for 6 hours. Pore size distributions, pore volumes, and BET isotherms were determined from N_2 adsorption-desorption experiments. The wall thicknesses were calculated as: $a_0 - \text{pore size}$ ($a_0 = 2 \times d(100)/\sqrt{3}$).

Block copolymer	Reaction temperature ($^\circ\text{C}$)	$d(100)$ (\AA)	BET surface area (m^2/g)	Pore size (\AA)	Pore volume (cm^3/g)	Wall thickness (\AA)
$\text{EO}_5\text{PO}_{70}\text{EO}_5$	35	118 (117)	630	100	1.04	35
$\text{EO}_{20}\text{PO}_{70}\text{EO}_{20}$	35	104 (95.7)	690	47	0.56	64
$\text{EO}_{20}\text{PO}_{70}\text{EO}_{20}$	35, 80^*	105 (97.5)	780	60	0.80	53
$\text{EO}_{20}\text{PO}_{70}\text{EO}_{20}$	35, 80^*	103 (99.5)	820	77	1.03	38
$\text{EO}_{20}\text{PO}_{70}\text{EO}_{20}$	35, 90^*	108 (105)	920	85	1.23	36
$\text{EO}_{20}\text{PO}_{70}\text{EO}_{20}$	35, 100^*	105 (104)	850	89	1.17	31
$\text{EO}_{17}\text{PO}_{55}\text{EO}_{17}$	40	97.5 (80.6)	770	46	0.70	47
$\text{EO}_{20}\text{PO}_{30}\text{EO}_{20}$	60	77.6 (77.6)	1000	51	1.26	39
$\text{EO}_{26}\text{PO}_{39}\text{EO}_{26}$	40	92.6 (88.2)	960	60	1.08	42
$\text{EO}_{13}\text{PO}_{70}\text{EO}_{13}$	60	80.6 (80.5)	950	59	1.19	34
$\text{PO}_{19}\text{EO}_{33}\text{PO}_{19}$	60	74.5 (71.1)	1040	48	1.15	34

*Reaction at 35°C for 20 hours, then heating to the higher temperature for 24 hours, or for the second entry for 80°C , 48 hours.

with hexagonal symmetry and large pore sizes (Fig. 3D).

This adjustment of the pore size of SBA-15 can be made essentially continuously by systematically varying the relative concentrations of swelling agent and copolymer or cationic surfactant species used in the respective reaction mixtures. Figure 6 shows the increases that occur in the XRD $d(100)$ spacings and the subsequent mean pore sizes as functions of the TMB:EO₂₀PO₇₀EO₂₀ mass ratio (ranging from 0 to 2) for SBA-15. Although the $d(100)$ spacing and pore size of MCM-41 prepared by using cationic surfactant can be expanded to 100 Å (4) by addition of TMB, the increase is much less than for SBA-15 (Fig. 6). Furthermore, the XRD patterns for MCM-41 materials with such expanded channel dimensions tend to consist of single low-angle peaks (4, 9), which reflect relatively poor mesoscopic ordering compared to that of SBA-15 (Fig. 5A). When the pore size of SBA-15 is expanded by using TMB as a cosolvent under otherwise identical conditions, the wall thickness remains unchanged, as does the hydrothermal stability of the resultant mesoporous product. Even for structures with pore sizes up to 300 Å, the materials retain their periodic structure after hydrothermal treatment.

The 31- to 64-Å-thick silica walls of SBA-15 impart significantly greater hydrothermal stability to calcined SBA-15 in comparison to calcined MCM-41 materials prepared without additional treatment with TEOS (27, 28). Calcined MCM-41, pre-

pared by using C₁₆H₃₃N(CH₃)₃Br as previously described (9), shows a well-resolved hexagonal XRD pattern (Fig. 7A), but after heating in boiling water for 6 hours, the material becomes amorphous and loses all XRD scattering reflections (Fig. 7B). In contrast to this, all of the calcined SBA-15 samples prepared with the triblock PEO-PPO-PEO copolymers are stable after heating in boiling water for 24 hours under otherwise identical conditions. The XRD pattern of calcined SBA-15 prepared with EO₂₀PO₇₀EO₂₀ at 35°C (Fig. 1B) is essentially unchanged from that obtained after the sample has been heated in boiling water for 24 hours (Fig. 7C). All scattering reflections are retained after this relatively severe hydrothermal treatment, although the (210) reflection becomes broader and the (300), (220), and (310) peaks become weaker. The (100) peak, however, is observed with similar intensity (Fig. 7C). BET measurements carried out after such hydrothermal treatment show that the monodispersity of the pore size, the high surface area, and the high pore volume are retained (29). By providing larger pores and more stable walls, the SBA-15 synthesis procedure is an improvement over two-step postsynthesis treatments that use TEOS to stabilize mesoporous MCM-41 by reinforcing the inorganic wall with additional silica (4, 28).

The ²⁹Si magic-angle spinning nuclear magnetic resonance spectrum (30) of as-synthesized hexagonal SBA-15 shows three broad peaks at 92, 99, and 109 ppm. These peaks correspond to Q², Q³, and Q⁴ silica species, respectively, which are associated with progressively increased silica cross-linking. From the relative peak areas, the ratios of these species are established to be Q² : Q³ : Q⁴ = 0.07 : 0.78 : 1. These results indicate that compared to MCM-41, SBA-15 has a somewhat less condensed, but similarly locally disordered, silica framework (7).

Thermal gravimetric and differential thermal analyses (TGA and DTA) in air of SBA-15 prepared with EO₂₀PO₇₀EO₂₀ show total weight losses of 58 weight %. At 80°C, TGA registers a 12 weight % loss accompanied by an endothermic DTA peak because of desorption of water (7, 12). This is followed by a 46 weight % TGA loss at 145°C, which coincides with an exothermic DTA peak associated with decomposition of the organic block copolymer (7, 12, 31).

The temperature (~145°C) at which the block copolymer species are decomposed and desorbed from the SBA-15 channels is much lower than the decomposition temperature of pure EO₂₀PO₇₀EO₂₀

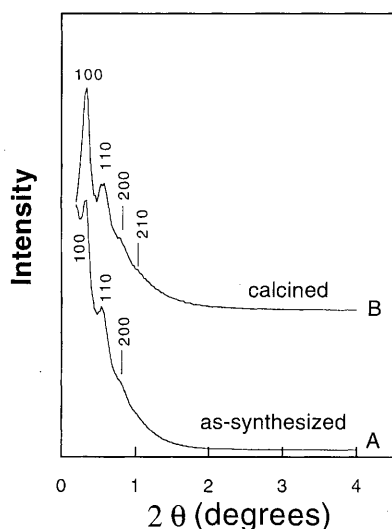


Fig. 5. Powder XRD patterns of (A) as-synthesized and (B) calcined mesoporous silica SBA-15 prepared using the amphiphilic triblock copolymer EO₂₀PO₇₀EO₂₀ with TMB added as an organic swelling agent. The chemical composition of the reaction mixture was 4 g copolymer:3 g TMB:0.041 mol TEOS:0.24 mol HCl:6.67 mol H₂O.

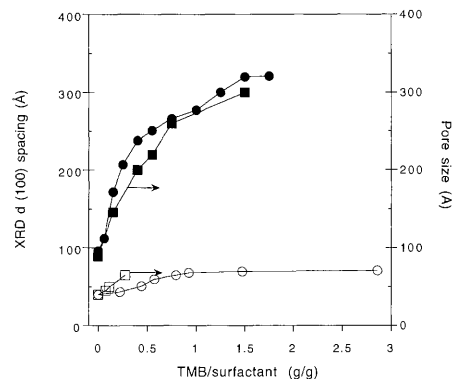


Fig. 6. Variation of the $d(100)$ spacings (circles) and pore sizes (squares) for hexagonal mesoporous SBA-15 (solid circles and squares) and for hexagonal mesoporous MCM-41 (open circles and squares) as functions of the TMB/surfactant ratio (g/g). The materials were calcined at 500°C in air for 6 hours before the XRD and adsorption measurements. Pore size data for MCM-41 were taken from (4), and the $d(100)$ spacing data from (6). The chemical composition of the reaction mixtures used to prepare the SBA-15 samples was 4 g EO₂₀PO₇₀EO₂₀ copolymer:x g TMB:0.041 mol TEOS:0.24 mol HCl:6.67 mol H₂O. The reaction mixture for the MCM-41 samples was NaAlO₂:5.3 C₁₆TMACl:2.27 TMAOH:15.9 SiO₂:x g TMB:1450 H₂O (C₁₆TMACl, cetyltrimethylammonium chloride; TMAOH, tetramethylammonium hydroxide). The solid lines have been added to guide the eye.

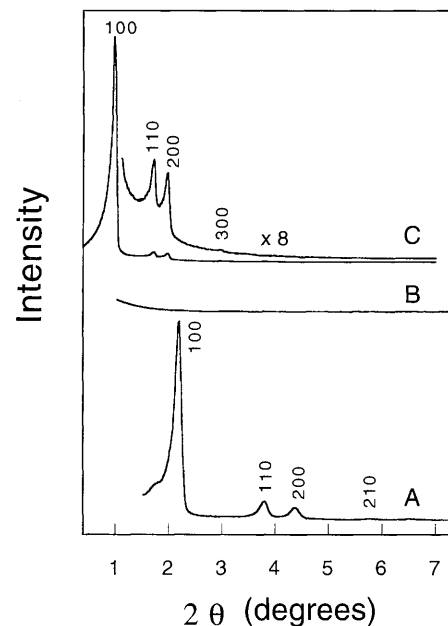


Fig. 7. Powder XRD patterns of (A) calcined MCM-41 silica prepared using the cationic surfactant C₁₆H₃₃N(CH₃)₃Br; (B) calcined MCM-41 after heating in boiling water for 6 hours; and (C) calcined SBA-15 prepared using the triblock copolymer EO₂₀PO₇₀EO₂₀ after heating in boiling water for 24 hours. The pattern in (C) is essentially unchanged from those shown (Fig. 1, A and B) for the as-synthesized and calcined SBA-15 products.

($\sim 250^\circ\text{C}$). It is also much lower than the temperature required ($\sim 360^\circ\text{C}$) to remove lower-molecular-weight cationic surfactant molecules from the channels of as-synthesized MCM-41 (7, 12). For comparison, the TGA of $\text{EO}_{20}\text{PO}_{70}\text{EO}_{20}$ impregnated in SiO_2 gel shows that the copolymer is not removed until 190°C ; the origin of the low decomposition temperature for poly(alkylene oxide) species in SBA-15 is currently under investigation. Alternatively, solvent extraction of as-synthesized SBA-15 using ethanol at 78°C allows the organic copolymer to be completely removed without decomposition, permitting its recovery and reuse. We have used such recycled copolymer species to synthesize high-quality hexagonal SBA-15 with characteristics and properties that are essentially identical to those presented above.

The structure-directed assembly of mesoscopically ordered silica by dilute poly(alkylene oxide) triblock copolymers in acid media likely occurs by a pathway that involves a combination of electrostatic and hydrogen-bonding interactions. Under acidic conditions, the PPO block is expected to display more hydrophobicity than the PEO block upon heating to 35° to 80°C (26), thereby increasing the tendency for mesoscopic ordering to occur. At $\text{pH} \approx 1$, positively charged protonated silicate species interact preferentially with the more hydrophilic PEO block or blocks to promote cooperative self-assembly of a silica-block-polymer-rich mesophase from a dilute water-rich phase (6, 8, 13). Concurrent and further condensation of the silica species in the presence of the block copolymer surfactant species results in the formation of the mesophase silica composite (6, 8, 9). The absence of sufficiently strong electrostatic or hydrogen-bonding interactions at pH values 2 to 7 leads to the formation of amorphous or otherwise disordered silica (11, 15). The use of amphiphilic block copolymers with higher molecular weights can be expected to yield materials with still larger pores than observed here, with potentially thicker walls and correspondingly enhanced hydrothermal stabilities.

In general, the silica poly(alkylene oxide) block copolymer systems described here represent a special case of a more general category of materials in which kinetically quenched structures are produced by using the self-assembly characteristics of block copolymers. Unlike conventional surfactants, block copolymers have the advantage that their properties can be nearly continuously tuned during synthesis by adjusting composition, molecular weight, or architecture. Moreover, they permit solution organization of large-

er-scale features than is possible with simple surfactants and achieve this at lower concentrations. For example, we have also prepared monoliths and highly ordered, oriented, continuous mesoporous silica thin films (pore size up to $\sim 90 \text{ \AA}$) on various substrates, by dip-coating using the block copolymers in organic solvents.

Other examples are found in purely organic systems, in which heterogeneous, nanoscale structures have been controllably produced and stabilized in block copolymer composites containing polymerizable additives. Hillmyer *et al.* have recently demonstrated this by selectively incorporating and cross-linking a thermosetting epoxy resin in the PEO domains of a poly(ethylene oxide)-poly(ethyl ethylene) (PEO-PEE) diblock copolymer (32). Novel morphologies can be produced by exploiting kinetically hindered microphase separations in such systems. Moreover, recent theoretical progress on the phase behavior of block copolymer/homopolymer blends is approaching a comprehensive understanding of the existence and sequence of mesoscopic morphologies obtained in these materials (33). The overall strategy is thus applicable not only to composites containing hydrophilic-hydrophobic copolymers, such as the silica-poly(alkylene oxide) system discussed above, but more generally to any self-assembling surfactant or copolymer system in which a network-forming additive is selectively partitioned among components. An enormous variety of nanophase-separated composite materials can be envisioned in which variations in the choice of blocks, copolymer compositions, or chain architecture are used to tune self-assembly, while processing variables such as temperature, pH , and external fields (34), are manipulated to regulate fixation of the one or more resultant structures.

REFERENCES AND NOTES

- M. E. Davis, *Chem. Ind.* **4**, 137 (1992).
- M. Estermann, L. B. McCusker, C. Baerlocher, A. Merroche, H. Kessler, *Nature* **352**, 320 (1991).
- C. T. Kresge, M. E. Leonowicz, W. J. Roth, J. C. Vartuli, J. S. Beck, *ibid.* **359**, 710 (1992).
- J. S. Beck *et al.*, *J. Am. Chem. Soc.* **114**, 10834 (1992).
- A. Sayari, *Chem. Mater.* **8**, 1840 (1996).
- Q. Huo *et al.*, *ibid.* **6**, 1176 (1994).
- Q. Huo, R. Leon, P. M. Petroff, G. D. Stucky, *Science* **268**, 1324 (1995).
- Q. Huo *et al.*, *Nature* **368**, 317 (1994).
- Q. Huo, D. I. Margolese, G. D. Stucky, *Chem. Mater.* **8**, 1147 (1996).
- D. M. Antonelli and J. Y. Ying, *Angew. Chem. Int. Ed. Engl.* **35**, 426 (1996); *Curr. Opin. Colloid Interface Sci.* **1**, 523 (1996); M. H. Lim, C. F. Blanford, A. Stein, *J. Am. Chem. Soc.* **119**, 4090 (1997); P. T. Tanev and T. J. Pinnavaia, *Science* **267**, 865 (1995); *ibid.* **271**, 1267 (1996).
- S. A. Bagshaw, E. Prouzet, T. J. Pinnavaia, *Science* **269**, 1242 (1995); E. Prouzet and T. J. Pinnavaia, *Angew. Chem. Int. Ed. Engl.* **36**, 516 (1997).
- C. Chen, H. Li, M. E. Davis, *Microporous Mater.* **2**, 17 (1993).
- D. Zhao *et al.*, in preparation.
- G. S. Attard, J. C. Glyde, C. G. Göltner, *Nature* **378**, 366 (1995).
- C. G. Göltner and M. Antonietti, *Adv. Mater.* **9**, 431 (1997); M. Antonietti and C. Göltner, *Angew. Chem. Int. Ed. Engl.* **36**, 910 (1997).
- A. Firouzi, F. Atef, A. G. Oertli, G. D. Stucky, B. F. Chmelka, *J. Am. Chem. Soc.* **119**, 3596 (1997).
- D. Khushalani, A. Kuperman, G. A. Ozin, *Adv. Mater.* **7**, 842 (1995).
- K. M. McGrath, D. M. Dabbs, N. Yao, I. A. Aksay, S. M. Gruner, *Science* **277**, 552 (1997).
- G. Wanka, H. Hoffmann, W. Ulbricht, *Macromolecules* **27**, 4145 (1994); B. Chu and Z. Zhou, in *Non-ionic Surfactants: Polyoxyalkylene Block Copolymers*, vol. 60 of *Surfactant Science Series V*, M. Nace, Ed. (Dekker, New York, 1996), p. 67.
- Pluronic poly(alkylene oxide) triblock copolymers are a trademarked product of BASF, Mt. Olive, NJ.
- The $\text{EO}_{106}\text{PO}_{70}\text{EO}_{106}$ triblock copolymer yields an $\text{Im}3\text{m}$ cubic ($a_0 = 176 \text{ \AA}$) silica mesostructure. The cubic phase assignments for silica-copolymer composites formed using $\text{EO}_{100}\text{PO}_{39}\text{EO}_{100}$ and $\text{EO}_{84}\text{PO}_{30}\text{EO}_{80}$ are based on 3D TEM studies. The space group is not yet assigned.
- D. Zhao, J. Feng, B. F. Chmelka, G. D. Stucky, data not shown.
- R. Schmidt, E. W. Hansen, M. Stöcker, D. Akporiaye, O. H. Ellestad, *J. Am. Chem. Soc.* **117**, 4049 (1995).
- P. J. Branton *et al.*, *J. Chem. Soc. Faraday Trans.* **90**, 2965 (1994).
- The average pore sizes estimated from the TEM image contrasts in Figs. 4, A and B, are slightly less than those determined from XRD and N_2 adsorption measurements.
- R. Zana, *Colloids Surf. A Physicochem. Eng. Aspects*, **123** 27 (1997).
- R. Ryoo and S. Jun, *J. Phys. Chem. B* **101**, 317 (1997); R. Ryoo, J. M. Kim, C. H. Ko, C. H. Shin, *ibid.* **100**, 17718 (1996).
- J. S. Beck, C. T. Chu, I. D. Johanson, C. T. Kresge, M. E. Leonowicz, W. J. Roth, J. C. Vartuli, S. B. McCullen, U.S. Patent 5,156,829 (1993).
- For example, for a calcined hexagonal SBA-15 sample with a pore size of 60 \AA , BET surface area of $780 \text{ m}^2/\text{g}$, and a pore volume of $0.80 \text{ cm}^3/\text{g}$ (Table 1), hydrothermal treatment in boiling water for 24 hours yields a material with an essentially identical XRD pattern, a pore size of 64 \AA , BET surface area of $690 \text{ m}^2/\text{g}$, and a pore volume of $0.79 \text{ cm}^3/\text{g}$.
- D. Zhao, N. Melosh, B. F. Chmelka, G. D. Stucky, data not shown.
- A Netzsch Thermoanalyzer STA 409 was used for thermal analysis of the solid products, simultaneously performing TGA and DTA with heating rates of 5 K min^{-1} in air.
- M. Hillmyer, P. M. Lipic, D. A. Hajduk, K. Almdal, F. S. Bates, *J. Am. Chem. Soc.* **119**, 2749 (1997).
- M. W. Matsen, *Macromolecules* **28**, 5765 (1995); _____ and M. Schick, *Curr. Opin. Colloid Interface Sci.* **1**, 329 (1996).
- I. A. Aksay *et al.* *Science* **273**, 892 (1996); A. Firouzi, D. J. Schaefer, S. H. Tolbert, G. D. Stucky, B. F. Chmelka, *J. Am. Chem. Soc.* **119**, 9466 (1997); S. H. Tolbert, A. Firouzi, G. D. Stucky, B. F. Chmelka, *Science* **278**, 264 (1997).
- Supported by NSF under grants DMR-9520971 (G.D.S.) and DMR-9257064 (B.F.C.), the U.S. Army Research Office under grant DAAH04-96-1-0443, and the David and Lucille Packard Foundation (B.F.C.). We made use of UCSB Materials Research Laboratory Central Facilities supported by NSF under award DMR-9632716. B.F.C. is a Camille and Henry Dreyfus Teacher-Scholar and an Alfred P. Sloan Research Fellow. We thank BASF (Mt. Olive, NJ) for providing block copolymer surfactants.

29 August 1997; accepted 14 November 1997